Journal of Biological Dynamics
Vol. 2, No. 1, January 2008, 40–54

Taylor & Francis
Taylor & Francis Group

Predation may defeat spatial spread of infection

Ivo Siekmann[a]*, Horst Malchow[a] and Ezio Venturino[b]

[a]*Institute of Environmental Systems Research, Department of Mathematics and Computer Science, University of Osnabrück, Osnabrück, Germany;* [b]*Department of Mathematics, University of Torino, Torino, Italy*

(*Received 04 January 2007; final version received 18 June 2007*)

A model of a phytoplankton–zooplankton prey-predator system with viral infection of phytoplankton is investigated. Virus particles (V) are taken into account by an explicit equation. Phytoplankton is split into a susceptible (S) and an infected (I) class. A lytic infection is considered, thus, infected phytoplankton cells stop reproducing as soon as the infection starts and die at an increased mortality rate. Zooplankton (Z) is grazing on both susceptible and infected phytoplankton following a Holling-type II functional response. After the local dynamics of the $V - S - I - Z$ system is analysed, numerical solutions of a stochastic reaction–diffusion model of the four species are presented. These show a spatial competition between zooplankton and viruses, although these two species are not explicitly coupled by the model equations.

Keywords: plankton; lytic viral infection; reaction–diffusion system; spatiotemporal structures; patchiness; multiplicative noise

1. Introduction

The importance of viruses for marine and especially phytoplankton ecology has been acknowledged in several recent publications [3–5,29,30,31,33]. Marine viral infections influence species diversity and gene transfer, furthermore, they are a major cause of phytoplankton mortality – it was shown that they are responsible for the sudden disappearance of algal blooms. By influencing the dynamics of phytoplankton which is the basis of all food webs in the sea, marine viruses play an even more important role, it is believed now that they are a key factor in global biogeochemical cycles.

Malchow *et al.* [17], Hilker and Malchow [8] and Hilker *et al.* [9] have analysed the influence of lysogenic and lytic phytoplankton infections on the local and spatio-temporal dynamics of a phytoplankton–zooplankton prey–predator system. Virus particles which cause the infectious disease are not modelled by an explicit dynamic equation. The transmission of the infection has been assumed as frequency-dependent [6,20,21].

Beretta and Kuang [1] have developed a dynamical model of virus particles that reproduce through lysis of infected phytoplankton cells with mass-action type of transmission. However, they consider neither space nor the effect of a predator grazing on phytoplankton.

*Corresponding author. Email: ivo.siekmann@uos.de

ISSN 1751-3758 print/ISSN 1751-3766 online

DOI: 10.1080/17513750801942552
http://www.informaworld.com

In this article, the approaches of Beretta and Kuang [1] are combined with the model in Malchow *et al.* [17] and Hilker *et al.* [9] in order to obtain a spatial prey–predator model with infected prey and explicit dynamics of viral particles. The Beretta–Kuang model is extended by a predator with Holling-type II functional response [11], *i.e.*, zooplankton grazing on both susceptible and infected phytoplankton. The standard Holling-type II prey–predator model has been studied extensively, cf. [14,24,26–28].

2. An extended Beretta–Kuang model

In 1998, Beretta and Kuang published a model of marine viral infections, which takes into account viral particles V by an explicit equation. Phytoplankton hosts are split into a susceptible class S and an infected class I:

$$\frac{\mathrm{d}V}{\mathrm{d}\tau} = -\lambda SV - m_V V + Bm_I I, \tag{1}$$

$$\frac{\mathrm{d}S}{\mathrm{d}\tau} = r_S S\left(1 - \frac{S+I}{K}\right) - \lambda SV, \tag{2}$$

$$\frac{\mathrm{d}I}{\mathrm{d}\tau} = \lambda SV - m_I I. \tag{3}$$

In this article, the parameters of (1–3) are retained. The model [1] is first extended by an equation describing the dynamics of the zooplankton Z grazing on phytoplankton with Holling-type II functional response [11]:

$$\frac{\mathrm{d}V}{\mathrm{d}\tau} = -\lambda SV - m_V V + Bm_I I, \tag{4}$$

$$\frac{\mathrm{d}S}{\mathrm{d}\tau} = r_S S\left(1 - \frac{S+I}{K}\right) - \lambda SV - a_S \frac{S}{H+S+I} Z, \tag{5}$$

$$\frac{\mathrm{d}I}{\mathrm{d}\tau} = \lambda SV - m_I I - a_I \frac{I}{H+S+I} Z, \tag{6}$$

$$\frac{\mathrm{d}Z}{\mathrm{d}\tau} = \frac{e_S a_S S + e_I a_I I}{H+S+I} Z - m_Z Z. \tag{7}$$

Susceptible phytoplankton reproduces logistically with growth rate r_S and carrying capacity K. Susceptible and infected phytoplankton both contribute to the competition term of the logistic growth. Free virus particles are denoted V. They infect the susceptible phytoplankton by transferring the genetic material into phytoplankton cells. The infection dynamics follows a mass action law with a transmission coefficient λ, *i.e.*, virus particles which infect the susceptible phytoplankton decrease at a rate of λSV, whereas susceptible phytoplankton passes over to the infected state at the same rate. The lytic infection starts as soon as a single virus particle has transferred its genetic material – the infected phytoplankton looses its capability of reproduction and dies at an additional disease-induced mortality rate m_I which is called as virulence. No quadratic competition term appears for infected phytoplankton I – intraspecific competition is neglected as the linear mortality m_I caused by the infection is considered more important. At the moment of lysis, reproduced virus particles are set free. This is taken into account by a replication factor B, which ranges from 10 up to 100, *i.e.*, on an average from 10 to 100 virus particles are reproduced by each phytoplankton cell which dies of lysis [25]. Zooplankton which is named Z feeds on both susceptible and infected phytoplankton with a Holling-type II functional response. A natural

mortality is accounted for by the linear mortality rate $-m_Z Z$. The predator is not susceptible to the infection, thus the equation for Z is not explicitly coupled with the equation for V. In order to simplify the following calculations, the model (4–7) is transformed to a dimensionless form. By assuming $e_Z := e_S = e_I$ and introducing the dimensionless variables

$$v = \frac{V}{K}, \quad s = \frac{S}{K}, \quad i = \frac{I}{K}, \quad z = \frac{Z}{e_Z K}, \quad t = \lambda K \tau,$$

the transformed system reads

$$\frac{\mathrm{d}v}{\mathrm{d}t} = -sv - \mu_V v + B\mu_I i =: f_V, \tag{8}$$

$$\frac{\mathrm{d}s}{\mathrm{d}t} = \rho_S s[\,1 - (s+i)\,] - sv - \alpha_S \frac{s}{1+\beta(s+i)} z =: f_S, \tag{9}$$

$$\frac{\mathrm{d}i}{\mathrm{d}t} = sv - \mu_I i - \alpha_I \frac{i}{1+\beta(s+i)} z =: f_I, \tag{10}$$

$$\frac{\mathrm{d}z}{\mathrm{d}t} = \frac{\alpha_S s + \alpha_I i}{1+\beta(s+i)} z - \mu_Z z =: f_Z, \tag{11}$$

with dimensionless parameters

$$\mu_V := \frac{m_V}{\lambda K}, \quad \mu_I := \frac{m_I}{\lambda K}, \quad \rho_S := \frac{r_S}{\lambda K}, \quad \beta := \frac{K}{H}, \quad \alpha_S = a_S \frac{e_Z}{\lambda H},$$
$$\alpha_I := a_I \frac{e_Z}{\lambda H}, \quad \mu_Z := \frac{m_Z}{\lambda K}.$$

In the following, $\alpha := \alpha_S = \alpha_I$ will be assumed in most cases.

Bhattacharyya and Bhattacharya [2] analyse a similar system, but with some important simplifications: The loss of virus particles due to infection is neglected, but included in our model. Furthermore, the model presented here is not restricted to the case when the zooplankton only feeds on the infected phytoplankton. For infected insects modelled in Bhattacharyya and Bhattacharya [2] this assumption might be justified. It is unlikely, though, that the differences in behaviour of susceptible compared with infected phytoplankton is the main reason for a phytoplankton cell to be fed by zooplankton. We assume that in the case of a coincidence of zooplankton and phytoplankton it depends more on chance than on the capability of the phytoplankton to escape if the predator is successful in catching the prey. Therefore, contrary to Bhattacharyya and Bhattacharya [2], the zooplankton grazes both on susceptible and infected phytoplankton without preference. The last difference is the lack of an additional density-dependent mortality rate in the zooplankton equation.

The second extension of the Beretta–Kuang model is the spatial spread of all populations, which is modelled by diffusion and the third is the accounting for environmental variability through multiplicative noise. Thus, we obtain the stochastic reaction–diffusion system

$$\frac{\partial v}{\partial t} = f_V(v,s,i) + \mathrm{d}\Delta v + v\omega\xi_v(x,y,t), \tag{12}$$

$$\frac{\partial s}{\partial t} = f_S(v,s,i,z) + \mathrm{d}\Delta s + s\omega\xi_s(x,y,t), \tag{13}$$

$$\frac{\partial i}{\partial t} = f_I(v,s,i,z) + \mathrm{d}\Delta i + i\omega\xi_i(x,y,t), \tag{14}$$

$$\frac{\partial z}{\partial t} = f_Z(s,i,z) + \mathrm{d}\Delta z + z\omega\xi_z(x,y,t), \tag{15}$$

where Δ is the Laplacian in two (horizontal) spatial dimensions (x, y). The eddy diffusion coefficient D is the same for all species, its non-dimensional form d is obtained by

$$d := \frac{D}{\lambda K L^2}. \tag{16}$$

The last terms at the right-hand sides stand for spatiotemporal white Gaussian noise with density-dependent intensity [17,18].

3. Analysis of the deterministic local dynamics

At first, the system of the ordinary differential equations (ODE) (8–11) is studied in order to understand the local dynamics. Stationary and oscillatory solutions are computed by a linear stability analysis. For the latter, we define

$$\tilde{K} := \frac{\mu_Z}{\alpha_S - \beta\mu_Z} \tag{17}$$

and

$$\gamma := \rho_S(1 - \tilde{K}) + \mu_I. \tag{18}$$

3.1. *Trivial and semi-trivial equilibria*

3.1.1. *Extinction* – $E_0 : (v^*, s^*, i^*, z^*) = (0, 0, 0, 0)$

As in [1], E_0 is an unstable saddle for all parametrizations.

3.1.2. *Disease-free equilibrium, extinction of* z – $E_s : (0, 1, 0, 0)$

For this stationary solution with extinction of both infection and predator, we have the stability condition

$$B < 1 + \mu_V. \tag{19}$$

as in [1]. This is proved by expanding the last row of the Jacobian, which leads to the additional constraint

$$\mu_Z > \frac{\alpha_S}{1 + \beta} \quad \text{or, equivalently } \tilde{K} \notin [0, 1]. \tag{20}$$

3.1.3. *Disease-free equilibrium* – $E_{s,z} : (0, s^*, 0, z^*(s^*))$

The system reduces to the well-known standard Holling-type II prey–predator model, cf. the references given in Section 1 The equilibrium is parametrized by

$$s^* = \frac{\mu_Z}{\alpha_S - \beta\mu_Z} = \tilde{K}, \qquad z^* = \frac{\rho_S}{\alpha_S}(1 - s^*)(1 + \beta s^*) = \frac{\rho_S}{\alpha_S}(1 - \tilde{K})(1 + \beta\tilde{K}) \tag{21}$$

The latter is feasible if it holds

$$\mu_Z < \frac{\alpha_S}{1 + \beta} \quad \text{or } \tilde{K} \in [0, 1]\,. \tag{22}$$

This shows that E_s and $E_{s,z}$ are mutually exclusive (cf. (20)).

Assuming $\alpha_S = \alpha_I =: \alpha$, we calculate the Jacobian

$$J_{(0,s^*,0,z^*)} = \begin{pmatrix} -s^* - \mu_V & 0 & B\mu_I & 0 \\ -s^* & \rho_S(1-2s^*) - \alpha\dfrac{z^*}{(1+\beta s^*)^2} & -\rho_S s^* + \alpha\beta\dfrac{s^*}{(1+\beta s^*)^2}z^* & -\alpha\dfrac{s^*}{1+\beta s^*} \\ s^* & 0 & -\mu_I - \alpha\dfrac{z^*}{1+\beta s^*} & 0 \\ 0 & \alpha\dfrac{z^*}{(1+\beta s^*)^2} & \alpha\dfrac{z^*}{(1+\beta s^*)^2} & -\mu_Z + \alpha\dfrac{s^*}{1+\beta s^*} \end{pmatrix}.$$

The matrix can be considerably simplified by substituting $\alpha(s^*/1+\beta s^*) = \mu_Z$ (cf. Equation (11)) and $\alpha(z^*/1+\beta s^*) = \rho_S(1-s^*)$ (cf. Equation (9)) as well as by using the definitions of $\tilde{K}$ (cf. Equation (17)) and γ (cf. Equation (18)).

$$J_{(0,s^*,0,z^*)} = \begin{pmatrix} -\tilde{K} - \mu_V & 0 & B\mu_I & 0 \\ -\tilde{K} & -\rho_S\tilde{K}\left(1-\beta\dfrac{1-\tilde{K}}{1+\beta\tilde{K}}\right) & -\rho_S\tilde{K}\left(1-\beta\dfrac{1-\tilde{K}}{1+\beta\tilde{K}}\right) & -\mu_Z \\ \tilde{K} & 0 & -\gamma & 0 \\ 0 & \rho_S\dfrac{1-\tilde{K}}{1+\beta\tilde{K}} & \rho_S\dfrac{1-\tilde{K}}{1+\beta\tilde{K}} & 0 \end{pmatrix}.$$

The characteristic polynomial of $J_{(0,s^*,0,z^*)}$ is a product of two quadratic polynomials:

$$p(x) = \left[x^2 + x(\tilde{K} + \gamma + \mu_V) + (\gamma\tilde{K} + \gamma\mu_V - \tilde{K}B\mu_I)\right] \times \left[x^2 + \rho_S\tilde{K}\left(1-\beta\frac{1-\tilde{K}}{1+\beta\tilde{K}}\right)x + \mu_Z\rho_S\frac{1-\tilde{K}}{1+\beta\tilde{K}}\right]. \tag{23}$$

We define,

$$p_1(x) := x^2 + x(\tilde{K} + \gamma + \mu_V) + (\gamma\tilde{K} + \gamma\mu_V - \tilde{K}B\mu_I), \tag{24}$$

$$p_2(x) := x^2 + \rho_S\tilde{K}\left(1-\beta\frac{1-\tilde{K}}{1+\beta\tilde{K}}\right)x + \mu_Z\rho_S\frac{1-\tilde{K}}{1+\beta\tilde{K}}. \tag{25}$$

The equilibrium $E_{s,z}$ is stable if all zeroes of p_1 and p_2 are negative. First, we investigate the zeroes of $p_1(x)$.

As $\tilde{K} + \gamma + \mu_V$ is always positive, this leads to

$$\gamma\tilde{K} + \gamma\mu_V - \tilde{K}B\mu_I > 0$$

or

$$B < \gamma\frac{\tilde{K} + \mu_V}{\mu_I\tilde{K}} = 1 + \mu_V\frac{\gamma}{\mu_I\tilde{K}} + \frac{\rho_S(1-\tilde{K})}{\mu_I}. \tag{26}$$

after substitution for γ. By analysing p_2, we get a second stablity condition for μ_Z: In p_2, the term $\mu_Z\rho_S(1-\tilde{K}/1+\beta\tilde{K})$ is always positive.

Thus, we get negative zeroes if

$$1 - \beta \frac{1 - \tilde{K}}{1 + \beta \tilde{K}} > 0$$

or by substituting for $\tilde{K}$:

$$\mu_Z > \frac{\alpha}{\beta} \frac{\beta - 1}{\beta + 1}. \tag{27}$$

This is the stability condition of the prey–predator model with Holling-type II functional response. If Equation (27) is not fulfilled a Hopf bifurcation occurs as in the prey–predator model without infection.

3.1.4. *Extinction of predator* $z - E_{v,s,i} : (v^*(s^*), s^*, i^*(s^*), 0)$

The parametrization of this equilibrium is

$$v^* = \rho_S \mu_I \frac{1 - s^*}{\mu_I + \rho_S s^*}, \quad s^* = \frac{\mu_V}{B - 1}, \quad i^* = \frac{s^*}{\mu_I} v^* = \rho_S s^* \frac{1 - s^*}{\mu_I + \rho_S s^*}. \tag{28}$$

This equilibrium is feasible if

$$B > 1 + \mu_V, \tag{29}$$

which means that this equilibrium appears when E_s is unstable.

By expanding the last row of the Jacobian, we get the constraint (in addition to the one computed by Beretta and Kuang [1], see below)

$$\mu_Z > \frac{\alpha_S s^* + \alpha_I i^*}{1 + \beta(s^* + i^*)}. \tag{30}$$

Assuming $\alpha := \alpha_S = \alpha_I$, we calculate

$$\begin{aligned} s^* + i^* &= \frac{s^*(\mu_I + \rho_S)}{\mu_I + \rho_S s^*} \\ &= \frac{\mu_I + \rho_S}{\mu_I / s^* + \rho_S} \\ &= \mu_V \frac{\mu_I + \rho_S}{(B - 1)\mu_I + \rho_S \mu_V} \end{aligned}$$

and by substituting into Equation (30) we get – again under the assumption that $\alpha_S = \alpha_I =: \alpha$:

$$\mu_Z > \alpha \frac{\rho_S + \mu_I}{\rho_S + (B - 1)/\mu_V \mu_I + (\rho_S + \mu_I)\beta}.$$

By solving for B, we compute the constraint:

$$B > 1 + \mu_V \frac{\gamma}{\mu_I \tilde{K}}. \tag{31}$$

Beretta and Kuang [1] have shown that for small values of s^* a Hopf bifurcation occurs. This can also be stated by means of B: As B increases above a certain threshold (which can be computed explicitly but leads to a very lengthy expression), the stationary solution passes over to a limit cycle.

3.2. *Non-trivial equilibrium ($E_{v,s,i,z}$)*

Also, the non-trivial stationary solution can be computed explicitly. However, there are strong indications that coexistence of viruses, susceptible and infected prey and the predator is only possible when the populations oscillate. A reason for this phenomenon can be found by looking at feasibility conditions for the non-trivial stationary solution.

Again, we assume $\alpha_S = \alpha_I = \alpha$ in this section. Using the definitions of $\tilde{K}$ (cf. Equation (17)) and γ (cf. Equation (18)) from above a carrying capacity $\tilde{K}$ of the phytoplankton population can be computed from Equation (11):

$$s^* + i^* = \frac{\mu_Z}{\alpha - \beta\mu_Z} = \tilde{K}. \tag{32}$$

By replacing $s^* + i^*$ by $\tilde{K}$, adding Equations (9) and (10) and solving $f_S + f_I = 0$ for z^*, we obtain

$$\begin{aligned} z^*(s^*, i^*) &= \frac{1}{\mu_Z}\left[\rho_S s^*(1 - \tilde{K}) - \mu_I i^*\right] \\ &= \frac{1}{\mu_Z}\left[(\gamma - \mu_I)\tilde{K} - i^*\gamma\right]. \end{aligned} \tag{33}$$

In Equation (33), s^* was replaced by $s^* = \tilde{K} - i^*$.

With Equation (33) and Equation (9), we calculate

$$i^* = \frac{\tilde{K}}{\gamma} v^*. \tag{34}$$

By solving $f_V = 0$ (cf. (8)) for i^* we receive,

$$i^* = \frac{\mu_V + \tilde{K}}{B\mu_I + v^*} v^*, \tag{35}$$

so that finally v^* can be computed:

$$v^* = \gamma\left(1 + \frac{\mu_V}{\tilde{K}}\right) - B\mu_I. \tag{36}$$

Now, we can state the complete non-trivial stationary solution:

$$v^* = \gamma\left(1 + \frac{\mu_V}{\tilde{K}}\right) - B\,\mu_I, \tag{37}$$

$$s^* = \tilde{K} - i^* = -\mu_V + \frac{B\,\mu_I\,\tilde{K}}{\gamma}, \tag{38}$$

$$i^* = \tilde{K} + \mu_V - \frac{B\,\mu_I\tilde{K}}{\gamma}, \tag{39}$$

$$z^* = -\gamma\,\frac{\mu_V}{\mu_Z} + \frac{(B-1)\,\mu_I\,\tilde{K}}{\mu_Z}. \tag{40}$$

This solution is feasible, if v^*, s^*, i^* and z^* are positive. Thus, feasibility conditions can be computed. Solving $v^* > 0$ (or $i^* > 0$) for B gives Equation (26), whereas $z^* > 0$ leads to

Equation (31). $s^* > 0$ gives a weaker condition than using $z^* > 0$ so that the range of feasibility is given by

$$1 + \mu_V \frac{\gamma}{\mu_I \tilde{K}} < B < 1 + \mu_V \frac{\gamma}{\mu_I \tilde{K}} + \frac{\rho_S(1-\tilde{K})}{\mu_I}. \tag{41}$$

Note that this is exactly the range where both $E_{s,z}$ and $E_{v,s,i}$ are stable. This may be a reason for the observation which can be made by numerical simulations that the coexistence solution is never attained (cf. Section 3.3).

3.3. *Summary of the stability analysis and numerical stability results*

In the preceding sections, it has been demonstrated that there are two independent stability conditions for all semi-trivial stationary solutions: One depends on B, the replication factor of the viruses, and the other one on μ_Z, the dimensionless mortality of the predator. Thus, stability ranges can be represented by surfaces in the $\mu_Z - B$ plane and the results of the stability analysis can be summarized in the parameter diagram shown in Figure 1. Furthermore, all results are shown in Table 1.

The equilibria which are stable according to the linear stability analysis are represented by different grey values. The analytical results are sufficient to predict the system behaviour in the right part of the parameter diagram. However, for values of μ_Z below the Hopf bifurcation point of $E_{s,z}$ the situation is not as clear: Numerical simulations show that the coexistence limit cycle as well as quasiperiodic and chaotic solutions exist in this area.

A look on Table 1 shows that the feasibility range of the non-trivial stationary solution $E_{v,s,i,z}$ coincides with the region where both $E_{s,z}$ and $E_{v,s,i}$ are stable (cf. Equations (26), (31) and (41), respectively). Extensive numerical experiments varying initial conditions showed that $E_{v,s,i,z}$ was

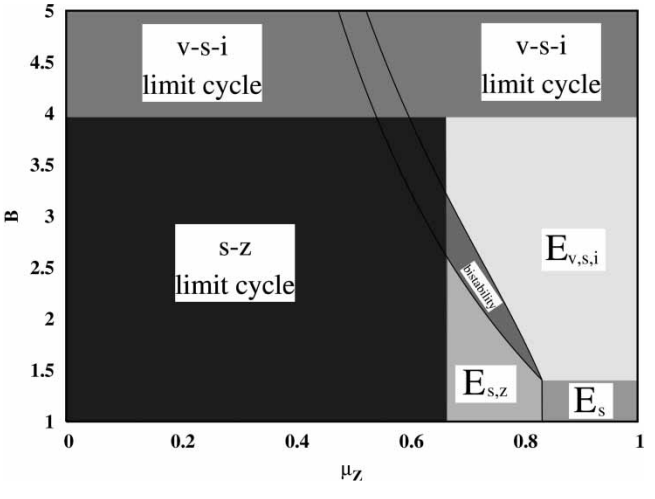

Figure 1. Depending on the replication factor B and the mortality rate μ_Z of the zooplankton the stability ranges of the stationary solutions are shown for the parameter values: $\rho_S = 1$, $\mu_V = 0.4$, $\mu_I = 1$, $\alpha = \alpha_S = \alpha_I = 5$, $\beta = 5$. This parametrization rather than the one given in Equation (42) was chosen to give an illustrative view of all facets of the system behaviour. For the parametrization proposed by Beretta and Kuang [1] the bistability area shrinks so much that it is not visible in the diagram. The mentioned region labelled 'bistable' admits either $E_{s,z}$ or $E_{v,s,i}$ to be reached depending on the initial conditions. On the other hand, in exactly this region the feasibility conditions of the non-trivial stationary solution $E_{v,s,i,z}$ are met. However, extensive numerical experiments show that the coexistence state $E_{v,s,i,z}$ is never reached. In the left part of the diagram, not only limit cycles of the subsystems s and z (extinction of the infection) or v, s and i (extinction of the predator) exist, but between the labels '$v - s - i$ limit cycle' and '$s - z$ limit cycle' there is also a region where a coexistence limit cycle appears.

Table 1. Summary of the analytical results of the stability analysis.

	Feasibility conditions		Stability constraints	
	B	μ_Z	B	μ_Z
E_s	—		$B < 1 + \mu_V$	$\tilde{K} \notin [0, 1]$
$E_{s,z}$	—	$\tilde{K} \in [0, 1]$	$B < 1 + \mu_V(\gamma/\mu_I\tilde{K}) + (\rho_S(1 - \tilde{K})/\mu_I)$	$\mu_Z > (\alpha/\beta)(\beta - 1/\beta + 1)$ (Hopf bif.)
$E_{v,s,i}$	$B > 1 + \mu_V$	—	$B > 1 + \mu_V(\gamma/\mu_I\tilde{K})$ B high (Hopf bif.)	
$E_{v,s,i,z}$	$1 + \mu_V(\gamma/\mu_I\tilde{K}) < B < 1 + \mu_V(\gamma/\mu_I\tilde{K}) + (\rho_S(1 - \tilde{K})/\mu_I)$		unknown	

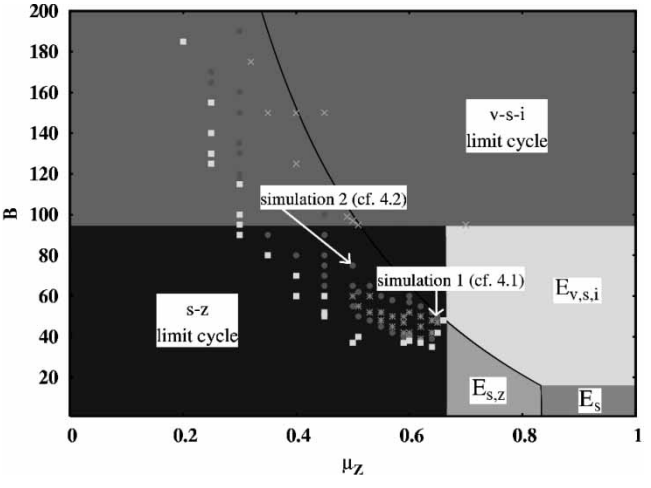

Figure 2. The parameter diagram for the parametrization given in Equation (42) shows for selected simulations with varying μ_Z and B which type of solution is attained. Reaching the $s - z$ limit cycle is displayed by bright squares, circles stand for $v - s - i - z$ oscillations, crosses ('x') represent oscillations of v, s and i, whereas asterisks ('*') indicate that the dynamics are more complex (multiply periodic, quasiperiodic, chaotic). The parametrizations of the two simulations in Section 4 are labelled.

never reached, though, in this range; merely either $E_{v,s,i}$ or $E_{s,z}$ were attained depending on the initial conditions.

However, as mentioned above, numerical simulations show that coexistence is nevertheless possible: If μ_Z is below the threshold for the Hopf bifurcation of $E_{s,z}$, oscillatory, quasiperiodic and chaotic coexistence solutions can be observed (Figure 2).

One example of a quasiperiodic solution is shown in Figure 3, a projection of the attractor to $v - s - z$ space is given in Figure 4.

4. Deterministic and stochastic spatial dynamics

After the investigation of the local dynamics the ODE Model, CF. Equations (4–7), is extended by admitting diffusive motion of all species, cf. from Equation (12–15). The parameter values proposed by Beretta and Kuang [1] were used for ρ_S, μ_V and μ_I. α_S, α_I, β, and the diffusion

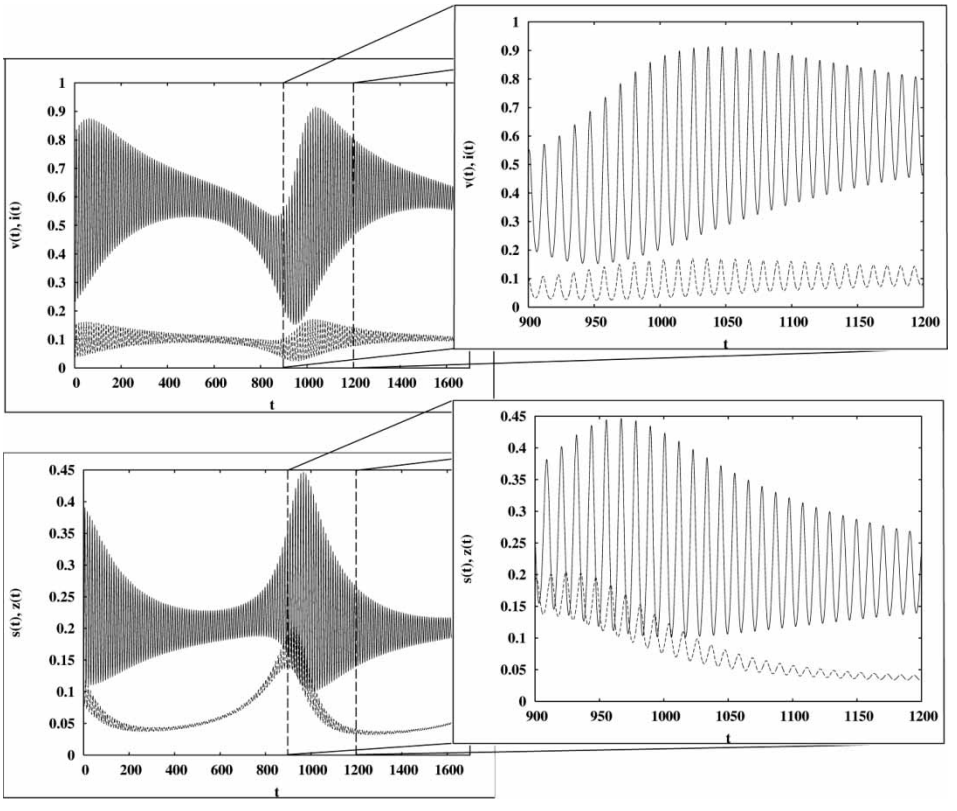

Figure 3. Quasiperiodic coexistence oscillations: Short time scale oscillations interfere with long time scale oscillations. Parametrization: $\rho_S = 1.0$, $\mu_V = 1.1$, $\mu_I = 1.07$, $\mu_Z = 0.6$, $\alpha_S = \alpha_I = 5.0$, $\beta = 5.0$ and $B = 7.09$.

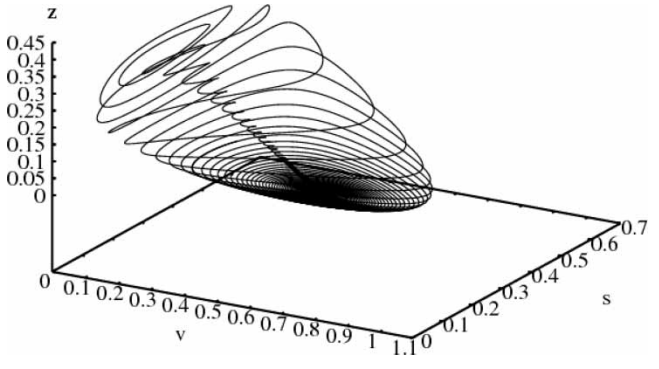

Figure 4. A projection of the quasiperiodic attractor to $v - s - z$ space. Parametrization: $\rho_S = 1.0$, $\mu_V = 1.1$, $\mu_I = 1.07$, $\mu_Z = 0.6$, $\alpha_S = \alpha_I = 5.0$ $\beta = 5.0$ and $B = 7.09$. Time interval: $t \in [8634.5, 10000]$.

coefficient d are chosen according to [16]:

$$\rho_S = 10, \quad \mu_V = 14.925, \quad \mu_I = 24.628, \quad \alpha_S = 5, \quad \alpha_I = 5, \quad \beta = 5, \quad d = 0.05. \quad (42)$$

The value of d has been chosen according to Okubo's diffusion diagrams (cf. [22]) in order to model processes on a kilometre scale. Numerical solutions were produced using finite differences for diffusion with an Euler scheme for reaction terms [32] and an Euler-Maruyama scheme [19] for the stochastic terms (cf. [12] and [7]). A series of figures is presented which summarizes

selected results of simulations. First, a 'weak' infection, which is characterized by a low level of the virus multiplication factor B, is presented. This type of a weak infection can go extinct due to an invasion of a predator, whereas a 'strong' infection with a higher value of B leads to the destruction of coherent structures and the emergence of a pattern which reminds of local infection herds.

4.1. *'Weak' infections go extinct*

First a weak infection with $\mu_Z = 0.65$ and $B = 49$, the other parameters chosen according to Equation (42), is considered. The results are shown in Figure 5.

Although the ODE model (12–15) reaches the coexistence limit cycle at arbitrary initial conditions the spatial model shows a different behaviour: In the first few timesteps, viruses and infected phytoplankton expand very quickly from the lower left patch (cf. Figure 5, $t = 5$ and $t = 15$) – note that the first two pictures are only 10 timesteps apart ! These waves consisting of viruses and both susceptibles and infected interfere and soon form a homogeneous distribution. Nevertheless, a small area in the centre occupied by phytoplankton and zooplankton cannot be intruded. This small patch expands very slowly, displacing the homogeneous distribution of v, s and i ($t = 570$) until nearly the whole space is disease-free. This leads to the paradoxical interpretation that the predator protects its prey from being infected.

The mathematical basis of this phenomenon can be found by a closer look at the local stability analysis. Apart from the $v - s - i - z$ limit cycle, also a limit cycle of the $s - z$ subsystem can be attained – if the initial values v_0 and i_0 of viruses and infected are set to zero (cf. Section 3.3). The spatial simulation shows that, in the model with diffusion, an $s - z$ patch is able to expand and displace the infection. This is accompanied by 'dynamic stabilization', cf. [15], of the stationary solution $E_{v,s,i}$: $E_{v,s,i}$ is unstable for the chosen parametrization (cf. Figure 2), nevertheless, a homogeneous predator-free distribution coinciding with the corresponding values of the stationary point $E_{v,s,i}$ remains stable for a certain time until it is displaced by the expanding patch of susceptibles and zooplankton.

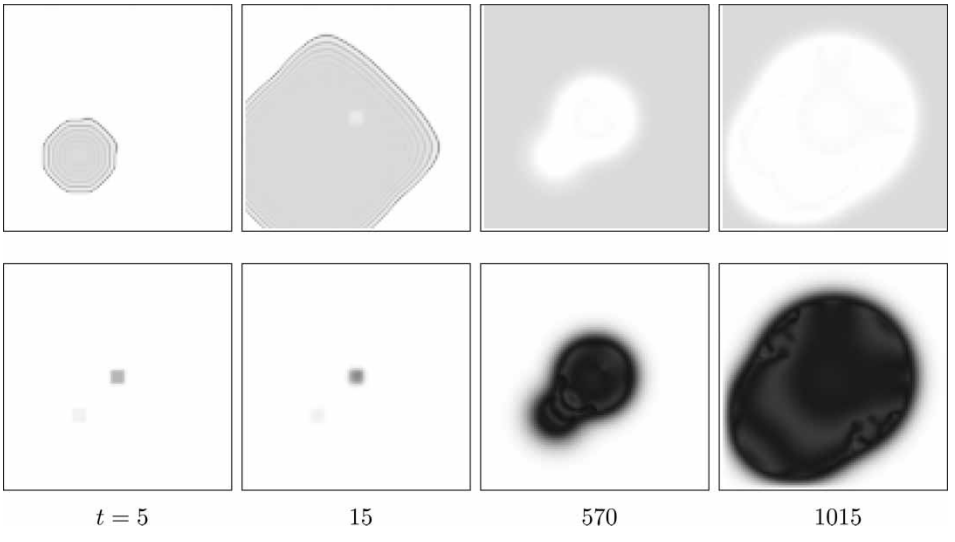

Figure 5. For $\mu_Z = 0.65$ and $B = 49$ the infection is displaced by the expanding zooplankton patch. For the other parameters cf. (42). Infected are displayed in upper, zooplankton in lower row. Initial conditions: One lower left patch with viruses, susceptibles and zooplankton, as well as one upper right patch with only susceptibles and zooplankton. Neumann boundary conditions. No noise.

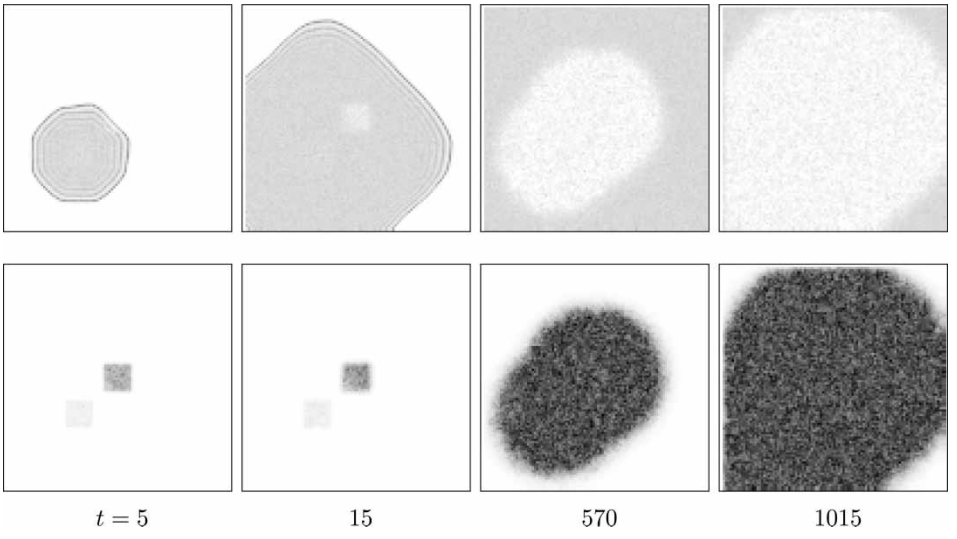

Figure 6. The same parametrization as in Figure 5. Stochastic environmental variability is accounted for by multiplicative noise with the intensity $\omega = 0.1$. Infected are displayed in upper, zooplankton in lower row. Initial conditions: one lower left patch with viruses, susceptibles and zooplankton, as well as one upper right patch with only susceptibles and zooplankton. Neumann boundary conditions.

Heuristically, this might be interpreted as similar phenomena, which have been studied in conjunction with front solutions: Owen and Lewis [23], Lewis and van den Driessche [13] and Hilker *et al.* [10] studied under which circumstances the direction of wave fronts of a population could be reversed. However, in our case, the situation is a bit more complicated: A stationary distribution of the $v - s - i$ subsystem is not invaded by a front, but by spiral waves of the $s - z$ subsystem.

If multiplicative noise is added, a stabilizing effect can be observed (cf. Figure 6): The expansion of the $s - z$ patch does not necessarily lead to the extinction of the infection. It has a certain non-vanishing survival probability. Furthermore, and as to be expected, the noise enhances the spatial spread of all species. Another effect of the noise is that the unrealistic regularity is blurred depending on the intensity ω of the added noise.

4.2. *'Strong' infection*

Choosing $\mu_Z = 0.5$ and $B = 75$ (for other parameters cf. Equation (42)) leads to a completely different situation: For a higher value of the replication factor B, the infection can establish in space (cf. Figure 7). Also, the position of this simulation in the parameter diagram, cf. Figure 2, is displayed.

In contrast to Figure 5, the zooplankton and susceptible phytoplankton are not able to form a virus-free area in the centre – virus particles 'invade' the area occupied by a small 'zooplankton island' ($t = 35$). This is again – as in the preceding subsection – accompanied by dynamic stabilization of $E_{v,s,i}$. Subsequently, the coherent structures dissolve, which is already visible at $t = 200$ in the plot for infected phytoplankton. At $t = 1000$, viruses and phytoplankton have produced an irregular pattern that reminds of local outbreaks. The small patches of local outbreaks are distributed over the whole area and vanish a short time after they occur. Zooplankton, however, still maintains a more or less coherent structure.

In this parametrization, the general features of the deterministic simulation are preserved after adding multiplicative noise. Therefore, figures are omitted.

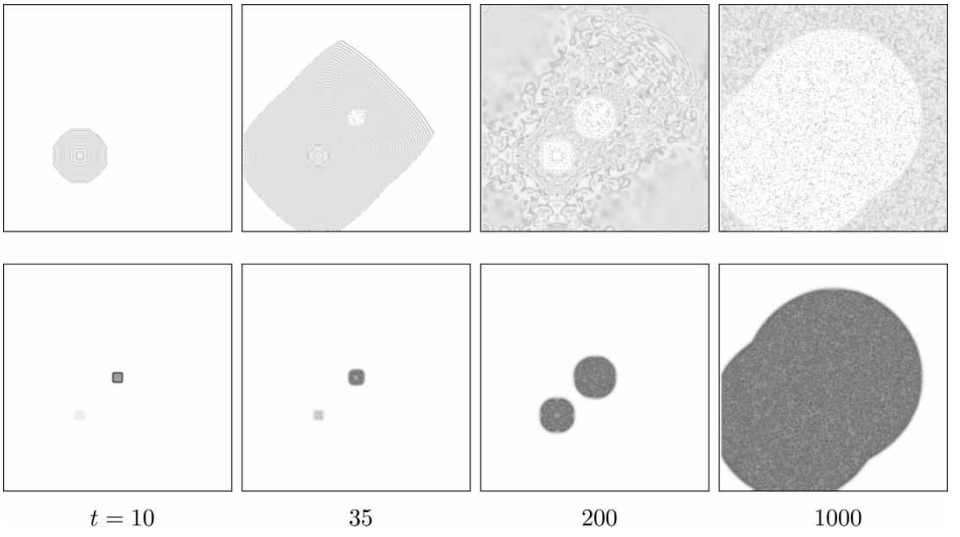

Figure 7. For $\mu_Z = 0.5$ and $B = 75$ the infection can establish in space. The complex pattern of i and z is characterised by local outbreaks of the disease. For other parameters cf. (42). Infected are displayed in upper, zooplankton in lower row. Initial conditions: One lower left patch with viruses, susceptibles and zooplankton, as well as one upper right patch with only susceptibles and zooplankton. Neumann boundary conditions.

5. Conclusions

In this article, a model of a prey–predator system with infected prey was studied. The complete analysis of the semitrivial stationary solutions of the local model revealed a complex interplay of the different subsystems – extinction of predator ($E_{s,z}$), extinction of infection ($E_{v,s,i}$), extinction of both predator and infection (E_S) – which could be well understood by representation in a parameter diagram depending on the mortality rate μ_Z of zooplankton and the replication factor B of viruses. As low levels of μ_Z can be interpreted as a greater strength of the predator, whereas high levels of B represent stronger infections, the system can thus be investigated under a given pressure of predation and infection. It was shown that there are parametrizations for which the system is bistable. In this range of parameters, either the $v - s - i$ subsystem (extinction of the predator) or the $s - z$ subsystem (extinction of the predator) are attained depending on the initial values. This range of parameters coincides with the feasibility range of the non-trivial stationary solution. However, the numerical analysis showed that only oscillatory solutions admit coexistence of viruses, susceptible and infected prey and the predator. Also, quasiperiodic and chaotic solutions exist for a certain range of parameters.

The numerical solution of the deterministic reaction–diffusion model with the parametrization of Section 4.1 shows a difference from the local model. For this parametrization, numerical solutions of the ODE system suggest that only the $v - s - i - z$ limit cycle can be attained independent of the initial values, but adding diffusion seems to destabilize the coexistence state. The $s - z$ subsystem is able to invade the whole space and displace the infection. The phenomenon of 'dynamic stabilization', which has been studied by Malchow and Petrovskii [15] can be observed for the $v - s - i$ subsystem: Although the stationary $v - s - i$ state is unstable it is 'stabilised' in the spatial model, *i.e.*, in a certain spatial area a 'plateau' of a homogeneous $v - s - i$ distribution is formed. In the long range, however, this state is displaced by the disease-free $s - z$ subsystem. In the given biological context, this can be interpreted as a biological invasion of an infected prey population by a predator. If the 'healing' effect of this invasion is realistic remains to be determined. However, predators are often considered to be responsible for infections going

extinct – usually assuming that it is easier for a predator to catch an infected than a susceptible individual. This decreases the reproduction rate of viruses so that the spread of the infection might be slowed down or even stopped. The result presented in this article shows that under certain circumstances a preference of predators for infected prey might not be necessary for the exctinction of an infection by predation. Adding multiplicative noise has a stabilizing effect – the complete extinction of the infection is prevented, if the noise level is above a certain threshold.

The other parametrization of the spatial model which is presented in Section 4.2 shows a different type of behaviour: Coherent structures dissolve and are replaced by local outbreaks of the disease. This behaviour of the model is characteristic for strong infections: an outbreak kills nearly all phytoplanktons in a certain region of space. Thus, the system collapses in a bounded area, but remains sensitive: as soon as the susceptible population has recovered the infection starts again. Therefore, the coherent structures dissolve and pass over to the local outbreak pattern. Adding multiplicative noise does not result in major changes of the model behaviour for this parametrization, but blurs artificial patterns of the deterministic simulation, which result in more realistic structures.

Future work shall include the replication of viruses in host cells.

Acknowledgements

The detailed suggestions of two anonymous referees are gratefully acknowledged.

References

[1] E Beretta and Y. Kuang, *Modeling and analysis of a marine bacteriophage infection*, Math. Biosci. 149 (1998), pp. 57–76.
[2] S. Bhattacharyya and D.K. Bhattacharya, *Pest control through viral disease: Mathematical modeling and analysis,* J. Theo. Biol. 238 (2006), pp. 177–197.
[3] G. Bratbak et al., *Virus production in Phaeocystis pouchetii and its relation to host cell growth and nutrition*, Aquat. Microb. Ecol. 16 (1998), pp. 1–9.
[4] J.A. Fuhrman, *Marine viruses and their biogeochemical and ecological effects*, Nature 399 (1999), pp. 541–548.
[5] J.A. Fuhrman and C.A. Suttle, *Viruses in marine planktonic systems,* Oceanography 6(2) (1993), pp. 51–63.
[6] H.W. Hethcote, *The mathematics of infectious diseases*, SIAM Rev. 42(4) (2000), pp. 599–653.
[7] D.J. Higham, *An algorithmic introduction to numerical simulation of stochastic differential equations*, SIAM Rev. 43(3) (2001), pp. 525–546.
[8] F.M. Hilker and H. Malchow, *Strange periodic attractors in a prey-predator system with infected prey,* Math. Popul. Stud. 13(3) (2006), pp. 119–134.
[9] F.M. Hilker et al., *Oscillations and waves in a virally infected plankton system. Part II: Transition from lysogeny to lysis*, Ecol. Complexity 3(3) (2006), pp. 200–208.
[10] ———, *Pathogens can slow down or reverse invasion fronts of their hosts*, Biol. Invasions 7 (2005), pp. 817–832.
[11] C.S. Holling, *Some characteristics of simple types of predation and parasitism,* Can. Entomologist 91(7) (1959), pp. 385–398.
[12] P.E. Kloeden and E. Platen, *Numerical Solution of Stochastic Differential Equations, Volume 23 of Applications of Mathematics*, Springer, Berlin, 1999.
[13] M.A. Lewis and P. van den Driessche, *Waves of extinction from sterile insect release,* Math. Biosci. 116 (1992), pp. 221–247.
[14] H. Malchow, *Spatio-temporal pattern formation in nonlinear nonequilibrium plankton dynamics*, Proceedings of the Royal Society of London B, 251:103–109, 1993.
[15] H. Malchow and S.V. Petrovskii, *Dynamical stabilization of an unstable equilibrium in chemical and biological systems*, Math. Comput. Model. 36 (2002), pp. 307–319.
[16] H. Malchow et al., *Numerical study of plankton-fish dynamics in a spatially structured and noisy environment*, Ecol. Model. 149 (2002), pp. 247–255.
[17] ——— et al., *Oscillations and waves in a virally infected plankton system. Part I: The lysogenic stage*, Ecol. Complexity 1(3) (2004), pp. 211–223.
[18] ——— et al., *Spatiotemporal patterns in an excitable plankton system with lysogenic viral infection,* Math. Comput. Model. 42(9–10) (2005), pp. 1035–1048
[19] G. Maruyama, *Continuous Markov processes and stochastic equations*, Rend. Circ. Mat. Palermo 4 (1955), pp. 48–90.
[20] H. McCallum, N. Barlow, and J. Hone, *How should pathogen transmission be modelled?* Trends Ecol. Evol. 16(6) (2001), pp. 295–300.

[21] A. Nold, *Heterogeneity in disease-transmission modeling,* Math. Biosci. 52 (1980), pp. 227–240.
[22] A. Okubo, *Oceanic diffusion diagrams,* Deep-Sea Res. 18 (1971), pp. 789–802.
[23] M.R. Owen and M.A. Lewis, *How predation can slow, stop or reverse a prey invasion,* Bull. Math. Biol. 63 (2001), pp. 655–684.
[24] M. Pascual, *Diffusion-induced chaos in a spatial predator-prey sys*tem, Proceedings of the Royal Society of London B, 251:1–7, 1993.
[25] L.M. Proctor and J.A. Fuhrman, *Viral mortality of marine bacteria and cyanobacteria,* Nature 343 (1990), pp. 60–62.
[26] M.L. Rosenzweig and R.H. MacArthur, *Graphical representation and stability conditions of predator-prey interactions*, Am. Nat. 97 (1963), pp. 209–223.
[27] M. Scheffer, *Fish and nutrients interplay determines algal biomass: a minimal model*, Oikos 62 (1991), pp. 271–282.
[28] J.H. Steele and E.W. Henderson, *A simple plankton model,* Am. Nat. 117 (1981), pp. 676–691.
[29] C.A. Suttle, A.M. Chan, and M.T. Cottrell, *Infection of phytoplankton by viruses and reduction of primary productivity*, Nature 347 (1990), pp. 467–469.
[30] C.A. Suttle, *Ecological, evolutionary, and geochemical consequences of viral infection of cyanobacteria and eukaryotic algae*, in *Viral Ecology,* C. J. Hurst, ed., Academic Press, San Diego, 2000, pp. 247–296.
[31] ———, *Viruses in the sea*, Nature 437 (2005), pp. 356–361.
[32] J.W. Thomas, *Numerical Partial Differential Equations: Finite Difference Methods. Volume 22 of Texts in Applied Mathematics*, Springer, New York, 1995.
[33] K.E. Wommack and R.R. Colwell, *Virioplankton: viruses in aquatic ecosystems*, Microbiol Mol Biol Rev, 64(1) (2000), pp. 69–114.